A 75-GHz Dynamic Antenna Array for Real-Time Imageless Object Detection via Fourier Domain Filtering

Daniel Chen[1], Stavros Vakalis[2], Jeffrey A. Nanzer[3]
Electrical and Computer Engineering, Michigan State University
[1]chendan7@msu.edu, [2]vakaliss@msu.edu, [3]nanzer@msu.edu

***Abstract*— We present a millimeter-wave dynamic antenna array operating at 75 GHz that can identify strong spatial Fourier domain artifacts in real-time for object detection without image reconstruction. Objects with sharp edges manifest broad-spectrum spatial frequency signals in the spatial Fourier domain that are located at angles orthogonal to the edge direction. The presented technique is based on active interferometry where noise transmitting sources are implemented to illuminate the scene of interest by mimicking thermal radiation. With rotational array dynamics, a one-dimensional (1D) array comprising of two transmitters and two receivers synthesizes a ring-shaped sampling function collecting sparse spatial Fourier information. In this way, broad-spectrum signals are captured, which can then be used for shape characterization. While the approach enables object classification, it does not sample enough information for full image reconstruction, which is beneficial for privacy preserving in contraband detection. We experimentally demonstrate the detection of simple objects with reduced information acquisition compared to full imaging systems.**

***Keywords*— Computational imaging, dynamic antenna arrays, interferometry, millimeter-wave radar, noise radar.**

I. Introduction

Sensing and imaging applications can benefit from the use of millimeter-wave systems due to the favorable characteristics of the wavelength of millimeter-wave signals. These include the fact that the wavelengths are short enough for good image resolution in many applications but are also long enough to propagate easily through fog, smoke, or garments [1], [2]. Interferometric imaging systems, which sample scene information in the Fourier spatial domain, have been of increasing interest recently due to their ability to generate high-resolution imagery using only a small fraction of the aperture area required for electronically- or mechanically-steered antennas and/or focal plane arrays [3], [4]. For most applications, image reconstruction is followed by a rigorous classification process to help identifying specific objects within the scene, such as concealed contraband [5], or military ground vehicles [6]. Furthermore, obtaining sufficient Fourier domain samples for full image reconstruction can be expensive for some applications, as additional receiving antennas might be required. However, various objects of common interest already manifest identifiable artifacts in the measuring spatial Fourier domain, particularly from man-made objects that comprise of discrete and sharp edges [7]. Direct detection of these signatures represents an opportunity for direct Fourier-domain object detection and classification without full images, removing the need for image reconstruction and classification algorithms, and requiring a small fraction of the amount of data that an imager requires.

We present an approach for imageless object identification using a 75-GHz dynamic antenna array. Rotated to collectively synthesize a unique spatial Fourier domain filter, the edge related strong spatial Fourier artifacts can be directly measured. The system is a freely rotating one-dimensional (1D) linear array comprising of two noise illuminating transmitters and a two-element interferometric receiving array. By dynamically rotating the array, a ring-shaped sampling function is generated in the spatial Fourier domain which captures the strong spatial Fourier responses induced by the sharp edges of objects in the scene. Previous works investigated Fourier-domain filtering at k_a-band [8], however the array in that work was large and bulky due to the longer wavelength, and furthermore did not operate in real-time. In this work, we experimentally demonstrate the ability to sample Fourier domain artifacts in real-time using a millimeter-wave dynamic array with the potential for a very compact physical implementation that is also amenable to portable operation.

II. Active Interferometric Imaging and Fourier Domain Artifacts

While interferometric imaging has traditionally been implemented with passive systems capturing thermal radiation, recent work has demonstrated the viability of actively illuminating a scene with noise to mimic thermal radiation while providing a significantly higher signal-to-noise ratio at the receiver [9]. The Fourier domain is often referred to as the *visibility* $V(u,v)$, where u and v are spatial frequencies. The visibility is the two-dimensional Fourier transform of the scene intensity $I(\alpha,\beta)$, where $\alpha = \sin\theta\cos\phi$ and $\beta = \sin\theta\sin\phi$ are the direction cosines, and is given by

$$V(u,v) = \iint_{-\infty}^{+\infty} I(\alpha,\beta) e^{j2\pi(u\alpha+v\beta)} d\alpha d\beta. \tag{1}$$

Conventional static interferometric imaging systems measure a subset of the available visibility as described by (1) which is defined by the sampling function

$$S(u,v) = \sum_{n=1}^{N}\sum_{m=1}^{M} \delta(u-u_n)\delta(v-v_m), \tag{2}$$

where $\delta(\cdot)$ is the Dirac delta function and $N \times M$ represents the maximum number of unique spatial frequency samples that

an interferometric array can measure. For a two-dimensional spatial Fourier plane (uv-plane), the specific u and v being sampled are dependent on the configuration of receiving antennas with respect to their spatial position x and y through $u = D_x/\lambda$ rad^{-1} and $v = D_y/\lambda$ rad^{-1}, where D_x and D_y are the receiver baselines in the spatial x and y dimensions for a given antenna pair and the signal wavelength $\lambda = c/f$.

Objects with sharp edges manifest broad spatial Fourier artifacts that are orthogonal to the physical edge direction and can be captured using a ring-shaped sampling function [7]. The artifacts of sharp edges are localized to narrow angles in the Fourier domain but extend radially outwards over a wide spatial frequency range. Thus, a ring-shaped filter centered at an offset spatial frequency can detect the angular locations of these responses, which can then be used to determine the approximate shape of the object by locating the angles of sharp edges. Most scenes produce spatial frequency signals with strong dc components, which may mask the broad-spectrum responses at low spatial frequencies. It is therefore typically beneficial to implement a spatial filter at a high enough spatial frequency to avoid the dc responses, but not so high that the spatial frequency artifacts have decreased in power.

The measured spatial frequency of a two-element array is determined by the electrical baseline of the antenna pair and is thus dependent on the physical separation and the wavelength of operation. Thus, for a given desired baseline to measure a specific spatial frequency, a system at low frequency will correspond to a physically large implementation. In contrast, by implementing the approach at a higher frequency, the same spatial Fourier domain frequency can be sampled with a smaller physical system. Implementing a ring-shaped sampling function using a static interferometric array is not only expensive but impractical due to spacing constraints. In contrast to the formulation of (2) where either additional receiving antennas or optimization of antennas placement are required to increase the unique spatial Fourier samples, a ring filter can be implemented by dynamically rotating a two-element interferometric antenna array, if the scene remains quasi-static during the measurement.

III. 75-GHz Dynamic Antenna Array

The experimental millimeter-wave dynamic antenna array is shown in Fig. 1. The system is a 1D array that comprises two noise transmitters and two receivers that are mounted on a freely rotating arm where the center of rotation is equidistant to the receivers and coupled to a motor encoder with 400 pulses per revolution (PPR) yielding an angle resolution of 0.9°. Furthermore, co-polarization is guaranteed by integrating both the transmitters and receivers on the same rotating arm. The array operates at 75 GHz and the intended spatial Fourier domain ring-shaped sampling function is obtained by rotating the system over a 180° span. The specific ring-shaped sampling function of the dynamic antenna array is thus given by

$$S_{ring}(u,v) = \sum_{k=0}^{K-1} \delta\left(u - u_k\right) \delta\left(v - v_k\right), \qquad (3)$$

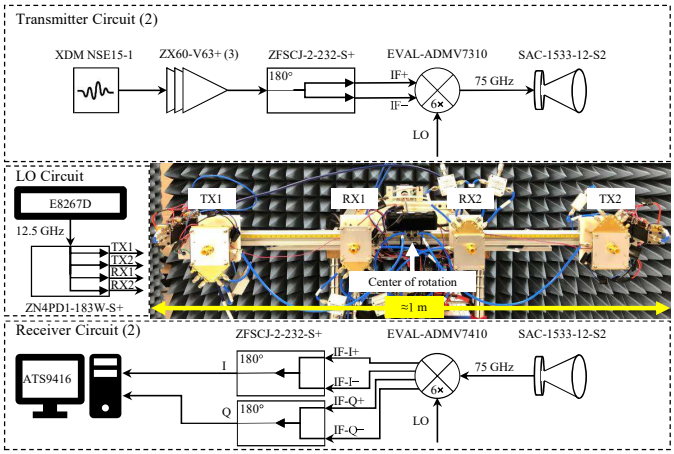

Fig. 1. Radio frequency schematics and photograph of the implemented 75 GHz dynamic antenna array. The noise sources are selected to accomplish spatio-temporally incoherent illumination of the scene. The upconverters and the downconverters enable a compact design with an overall span of slightly less than 1 m at millimeter-wave bands (i.e., 75 GHz) due to their 6× LO multiplier. Top: Schematic of one transmitter circuit. Middle Left: Schematic of the 12.5 GHz local oscillator circuit. Middle Right: Photo of the implemented 75 GHz dynamic antenna array. Bottom: Schematic of one receiver circuit. Number in parenthesis indicates the quantity I: In-phase. Q: Quadrature. IF: Intermediate frequency. LO: Local oscillator. TX: Transmitter. RX: Receiver.

where K is the number of angles over a 180° rotation, $u_k = D_\lambda \sin\gamma(k)$ and $v_k = D_\lambda \cos\gamma(k)$ represent the (u,v) information being sampled due to the implemented baseline D_λ and the discrete rotational angles $\gamma(k)$.

For each of the two transmitter circuits, a -66.9 dBm noise source with a bandwidth of 10–1600 MHz (RF-Gadgets XDM NSE15-1) is fed through three cascaded baseband amplifiers (Mini-Circuits ZX60-V63+) to obtain a power of -4.2 dBm. The amplified baseband noise is further fed into a 180° coupler (Mini-Circuits ZFSCJ-2-232-S+) to drive the intermediate frequency (IF) differential in-phase (I) ports of a upconverter (Analog Devices EVAL-ADMV7310) where its differential quadrature (Q) ports is terminated to 50 Ω. The upconverter is a fully integrated system in package (SiP) with 35 dB conversion gain and is desirable for its integrated 6× local oscillator (LO) feature where a 12.5 GHz LO is designed to mix with the baseband noise to generate a 75 GHz carrier that is immediately available to the upconverter's WR-12 waveguide back plate. Attached to the upconverter's waveguide is a 15 dBi conical horn antenna (Eravant SAC-1533-12-S2) with 30° E-plane beamwidth. Each of the two receiver circuits comprises the same 15 dBi conical horn antenna from Eravant that is mounted to a downconverter's WR-12 waveguide back plate (Analog Devices EVAL-ADMV7310). The downconverter is also a SiP with integrated low noise amplifier (LNA) that has 13 dB conversion gain and outputs differential I and Q signals. A 180° coupler (Mini-Circuits ZFSCJ-2-232-S+) is connected to the differential I and Q ports of the downconverter to provide the I/Q signals for processing. The implementation of the specific mixers enable the dynamic antenna array to be experimentally feasible at

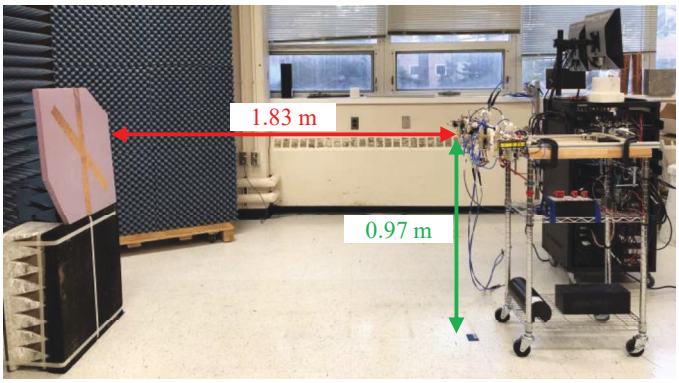

(a)

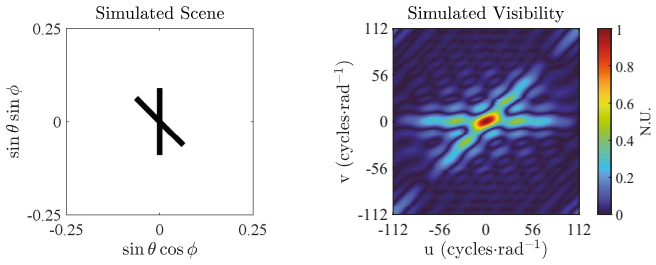

(b) (c)

Fig. 2. (a) Measurement setup of the two-stripe target that is 1.83 m away from the broadside of the 75 GHz dynamic antenna array with height of 0.97 m measured from its center of rotation to the floor. (b) Simulated scene of the two-stripe target where a 45° acute angle is formed and its intersection of the two stripes is aligned to the array's center of rotation. Each stripe has a physical dimension of 5.1 cm × 61.0 cm. (c) Simulated visibility. N.U.: Normalized Units.

millimeter-wave bands and compact where the dimension of the 1D array is slightly less than 1 m. The four required LO signals, designed at 12.5 GHz are generated using an Agilent PSG E8267D vector signal generator at 20 dBm to balance the total loss due to cabling and a four-way splitter (Mini-Circuits ZN4PD1-183W-S+) such that the available LO power at each mixer is approximately 4 dBm. The two pairs of I/Q baseband signals are captured by a desktop computer based digitizer (AlazrTech ATS9416), which supported real time data acquisition and signal processing, facilitating real time plotting of the filtered visibility samples.

IV. Experimental Evaluation

Experimental measurements were conducted in a semi-enclosed anechoic environment with the target placed 1.83 m from the 75 GHz dynamic antenna array, as shown in Fig. 2(a). The dynamic antenna array had a height of 0.97 m considering from its center of rotation to the floor. The two-stripe target was fabricated by arranging strips of copper tape to form a 45° acute angle on a foam board. Each copper stripe had dimensions of 5.1 cm × 61.0 cm. The foam board is effectively transparent at 75 GHz which allows the creation of identifiable spatial Fourier artifacts. The sharp edges from each of the two distinct stripes manifest broad spatial spectral Fourier responses that are orthogonal

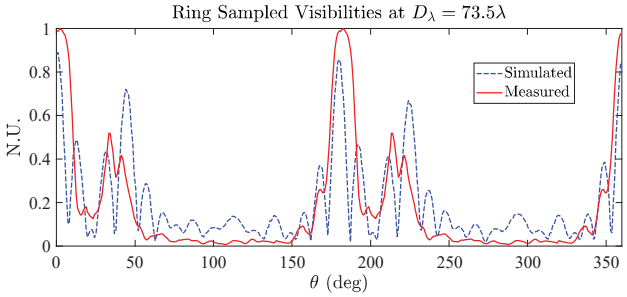

Fig. 3. Simulated and the measured ring sampled visibilities at a receiver baseline of $D_\lambda = 73.5\lambda$. The parameter θ represents the angle from the positive u-axis on the uv-plane in counter-clockwise direction. Referring to Fig. 2(c), a spatial Fourier ring-shaped sampling function of a receiver baseline of $D_\lambda = 73.5\lambda$ is expected to capture the edge induced artifacts at 0°, 45°, 180°, and 225° as indicated by the simulated blue dashed line. The angular location of the artifacts were verified with the measurement which is shown in solid red line. N.U.: Normalized Units

to the direction of the corresponding edges stripe as shown by the simulated target and its simulated spatial frequency responses shown in Fig. 2(b) and (c). The 1D dynamic antenna array was rotated 180° synthesizing a complete ring-shaped sampling function that covers the full 360° for the designed receiver baseline at 73.5λ since the visibility is symmetric. Simulated ring sampled visibilities obtained from a ring filter applied to Fig. 2(c) at a receiver baseline of $D_\lambda = 73.5\lambda$ is shown with the dashed blue lines in Fig. 3. The expected spatial Fourier artifacts that are induced by the physical edge of the two-stripe target are expected to appear at $\theta = \{0°,\ 45°,\ 180°,\ 225°\}$ where θ represents the angle with respect to the positive u-axis of the uv-plane in the counter-clockwise direction. The measured result for the same receiver baseline is shown in red where the angular locations of the expected strong spatial Fourier artifacts closely match to the simulated result.

V. Conclusion

We demonstrated a 75-GHz dynamic antenna array for measuring the Fourier domain artifacts of objects for imageless object detection and classification. In contrast to prior work, the 75 GHz array demonstrated in this paper operated in real time and requires significantly less physical space for operation. Furthermore, the array was built using commercially available components. We experimentally verified the identification of unique spatial Fourier artifacts linked to object's physical feature in real time without requiring full image reconstruction. Since the approach does not acquire sufficient information for full image reconstruction, the approach supports the potential for object identification in privacy-preserving applications. These results may prove useful in object detection applications where real-time image-free detection with minimal data acquisition is beneficial, such as contraband detection.

REFERENCES

[1] N. Currie and C. Brown, *Principles and Applications of Millimeter-Wave Radar*. Artech House, 1987.

[2] J. A. Nanzer, *Microwave and Millimeter-Wave Remote Sensing for Security Applications*. Artech House, 2012.

[3] Y. Álvarez, Y. Rodriguez-Vaqueiro, B. Gonzalez-Valdes, F. Las-Heras, and A. García-Pino, "Fourier-Based Imaging for Subsampled Multistatic Arrays," *IEEE Trans. Antennas Propag.*, vol. 64, no. 6, pp. 2557–2562, Jun. 2016.

[4] E. Kpré, C. Decroze, M. Mouhamadou, and T. Fromenteze, "Computational Imaging for Compressive Synthetic Aperture Interferometric Radiometer," *IEEE Trans. Antennas Propag.*, vol. 66, no. 10, pp. 5546–5557, Oct. 2018.

[5] S. Stanko, D. Notel, A. Wahlen, J. Huck, F. Kloppel, R. Sommer, M. Hagelen, and H. Essen, "Active and passive mm-wave imaging for concealed weapon detection and surveillance," in *2008 33rd International Conference on Infrared, Millimeter and Terahertz Waves*, 2008, pp. 1–2.

[6] J. P. P. Gomes, J. F. B. Brancalion, and D. Fernandes, "Automatic Target Recognition in Synthetic Aperture Radar image using multiresolution analysis and classifiers combination," in *2008 IEEE Radar Conference*, 2008, pp. 1–5.

[7] D. Chen, S. Vakalis, and J. A. Nanzer, "Dynamic Antenna Array Design for Scene Classification Through Fourier-Domain Filtering," *IEEE Trans. Antennas Propag.*, vol. 69, no. 9, pp. 5953–5962, Sep. 2021.

[8] ——, "Imageless Shape Detection Using a Millimeter-Wave Dynamic Antenna Array and Noise Illumination," *IEEE Transactions on Microwave Theory and Techniques*, vol. 70, no. 1, pp. 758–765, 2022.

[9] S. Vakalis, D. Chen, and J. A. Nanzer, "Millimeter-Wave Imaging at 652 Frames per Second," *IEEE Journal of Microwaves*, pp. 1–9, 2021.